



A novel methodology for the diffusion coefficient determination in porous media by X-ray high-resolution radiographies

M. Santini^{1,a} , S. Fest-Santini¹, G. E. Cossali¹, N. Casatta², C. Lupo²

¹ Department of Engineering and Applied Sciences, University of Bergamo, Viale Marconi 5, 24044 Dalmine, BG, Italy

² Innovation Department, Diapath S.P.A., Via Pietro Savoldini 71, 24057 Martinengo, BG, Italy

Received: 9 December 2023 / Accepted: 22 July 2024

© The Author(s) 2024

Abstract The first step in diagnosing a patient with cancer is the biopsy and the study of the tissue sample taken, suitably processed, is essential for a correct diagnosis. Tissue processors are machines that automatically perform the entire processing protocol, often relying on empirical timing related to chemical diffusions in the biological samples. The determination of the diffusion coefficient in porous materials, such as histological tissue, is still under study with multiple methods often resulting in inaccurate predictions and with few amounts of literature data for biological samples. The authors present an experimental technique, based on a multitude of X-ray radiographs acquired over time, where the intensity of the attenuation to the ionising beam is proportional to the concentration of the solvent that diffuses in the histological preparation. The paper so describes a *proof-of-concept* of a novel method to estimate the diffusion coefficient in a histological sample, based on the acquisition of time-dependent X-ray radiographs and the solution of an inverse diffusion problem.

1 Introduction and motivations

The World Health Organisation (WHO) estimates that nearly every family in the world is affected by cancer, causing nowadays one in six deaths worldwide. The first step to diagnose a patient with cancer is the removal of a small amount of tissue (by biopsy or surgical procedure); the study of the removed histological specimen is crucial for the correct diagnosis; and therefore, it has a high impact in the survival rates.

The objective of histological specimen is to help infer a diagnostic through the performance of different tests standardised in protocols, such as the haematoxylin and eosin (H&E) staining histopathology protocol, immunohistochemistry (IHC) interpretation or molecular morphology (MOL). However, histological specimen must be accordingly processed and treated before a pathologist can analyse them and get a diagnostic conclusion.

2 Current state-of-the-art in histological specimen processing

Histological specimen processors are machines that carry out the entire processing protocol automatically, from formalin fixation to paraffin permeation. Modern processors are equipped with tanks containing the reagents which direct the different liquids into a thermo-vacuum-controlled processing chamber.

Unfortunately, the time necessary for each sample to be correctly and completely perfused is only estimated based on experimental tests and is strongly dependent on the type of organ and the size of the histological sample extracted.

An urgent need is to know the diffusion coefficient of the various solvents for each specific type of organ. There are no generalised references in the literature.

Having a better estimation of the coefficient of diffusion will optimise the tissue process, which may reduce the steps with respect to the current process, decreasing both the amount of chemicals and time required while decreasing the possibility of failure in every step.

Indeed, compromission risks will hopefully be reduced for the human diagnostic tissue (unique and unrepeatable samples): during tissue processing, the high number of chemicals used in the current system implies the possibility of failure in every single step of the process.

^a e-mail: maurizio.santini@unibg.it (corresponding author)

Fig. 1 Pork liver biopsy **a**, specimen exposed to X-rays **b** and **c** high-resolution radiography, in evidence the vascularization and the attenuation of intensity as the total thickness of the cylindrical histological sample varies

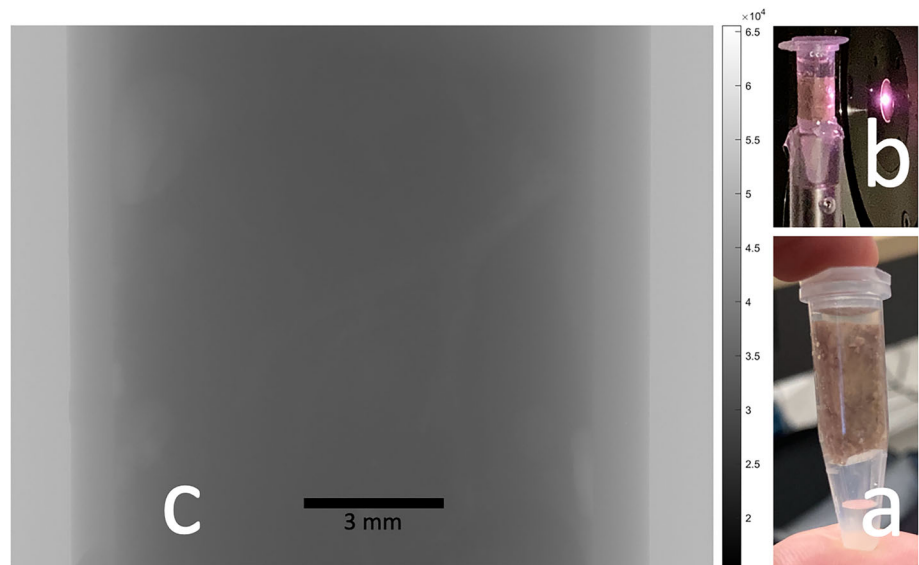
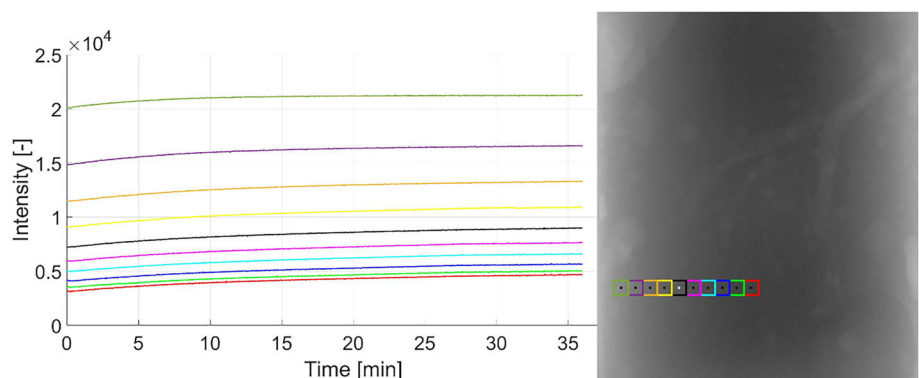


Fig. 2 X-ray grey-level intensity attenuation (pixel value) at different radial distance versus time (figure left) as obtained by the high-resolution radiography in 10 aligned ROIs (figure right)



Additionally, this reduces time in dehydration step because the removal of water from the tissue is less time-consuming. The normal processing needs at least 11 hours to be completed, which involves: the permeation of the tissue in liquid phase with alcohol and the subsequent permeation with xylene (due to the lack of affinity between the final encapsulation in paraffin and alcohol).

3 A proof-of-concept of a novel method to estimate the diffusion coefficient in a histological sample

The paper presents a *proof-of-concept* of a novel, non-invasive, method to estimate the diffusion coefficient based on the sequential recording of high-resolution radiographic images of a histological sample during the perfusion over time of a solvent (see Fig. 1). This method, applicable for porous media and cellular tissues [1], allows obtaining a measure of the (limited) density variation correlated to the X-ray intensity attenuation within the sample (see Fig. 2). The technique has the advantage of avoiding any modification of the sample, including the absence of any type of sensor or other measurement device in contact with the biological material, which can therefore undergo all the treatments foreseen by the processing protocol for an effective diagnosis.

The method is based on the solution of an inverse problem, using the data obtained from the experiments. The concentration of the diffusing species is determined by measuring the density variation as described in Sects. 3.1 and 3.2. A simplified model for the diffusion [2] of the solvent through the sample is proposed based on an analytical solution to the diffusion equation in cylindrical coordinates, as described in Sect. 4. The model outcomes are then used to extract the values of an average diffusion coefficient (D) from the data.

3.1 Experimental conditions

The presented experiment analyses the first step of the typical preparation reagents protocol for histological samples (see Table 1) based on the perfusion of the solvent (alcohol 70%) in the sample already stabilised in buffered formalin (standard method of tempering histological samples). For the experimental tests, a quasi-cylindrical sample (358 mg) of pork liver was used, placed in a

Table 1 A typical preparation reagents protocol for histological samples

^a Repeated 3 times
^b Repeated 2 times

	Alcohol 70%	Alcohol 95%	Alcohol ^a 100%	Xylene ^b	Paraffin <i>melted</i>	[min]
Processing time	30	45	60 × 3	90 × 2	60 × 3	615

1.5 mL Eppendorf in which the alcoholic solvent was injected by means of a Pasteur pipette with capillary stem, thus realistically simulating one of the standard processing phases.

The sample was then exposed to the ionising radiation in a custom microCT facility [3] by a microfocus X-ray source with conical emission (Hamamatsu L11091), typically operated at 120 kV and 50 μA. Due to the density of samples, fluids involved in the processing and container made of polymeric material used, artefacts due to hardening of the X-ray beam are negligible and therefore no additional filtration was used. The radiographs were acquired at a scan-rate of 1 Hertz for a total time of 30 min, recorded and digitalised as TIFF images with an X-ray digital detector PerkinElmer XRD 1611 (single substrate amorphous silicon active TFT/diode array type with direct deposition CsI:TI) having a pixel size of 100 μm with a total size of 4096 × 4096 pixels, at 16 bits (equal to 65,536 grey-levels). Distances between the X-ray source and the sample (SOD) and between the X-ray source and the detector (SDD) were, respectively, 20.2 mm and 400 mm. Subsequently, radiographs were processed to optimise the contrast and define the diffusion’s ROI (region of interest) within the sample, then were processed using a MATLAB® code developed by the authors (within the sample).

3.2 Radiographic images post-processing

Radiographies were corrected for charge accumulation of the X-ray digital detector, the so called “dark-field” optimisation and subsequently normalised by “bright-field” correction. The latter adjusts the non-uniform radiography acquisition system response of the sensitivity and the Gaussian density X-ray flux distribution due to the conical emission. These normalised radiographies of the tissue sample were used for all further image analysis. Since pixel dimensions needs to be converted in micrometric scale for calculate the dimensional diffusion coefficient, the resolution of the radiographies was determined with a metrological calibration and found to be 5.05 μm/pixel, in the present experiment.

4 Mathematical model

The diffusion equation in cylindrical coordinates, assuming the isotropy of the material and axial symmetry can be written as

$$\frac{\partial \rho}{\partial t} = D \left[\frac{\partial^2 \rho}{\partial r^2} + \frac{1}{r} \frac{\partial \rho}{\partial r} + \frac{\partial^2 \rho}{\partial z^2} \right] \tag{1}$$

where $\rho(r,z,t)$ is the concentration of the diffusing species and D is the diffusion coefficient. The initial (IC) and boundary (BC) conditions can be imposed assuming an initial uniform value of the concentration, ρ_0 , and a uniform and constant value of the concentration, ρ_1 , on the sample boundaries for $t > 0$. Introducing the non-dimensional quantity

$$\chi = \frac{\rho - \rho_1}{\rho_0 - \rho_1} \tag{2}$$

Equation (1) transforms to

$$\frac{\partial \chi}{\partial t} = D \left[\frac{\partial^2 \chi}{\partial r^2} + \frac{1}{r} \frac{\partial \chi}{\partial r} + \frac{\partial^2 \chi}{\partial z^2} \right] \tag{3}$$

The initial condition is now

$$\chi(r, z, 0) = 1 \tag{4}$$

while, the Dirichlet BC on the sample surface are

$$\chi(R_0, z, t) = 0; \quad \chi(r, z_0, t) = 0; \tag{5}$$

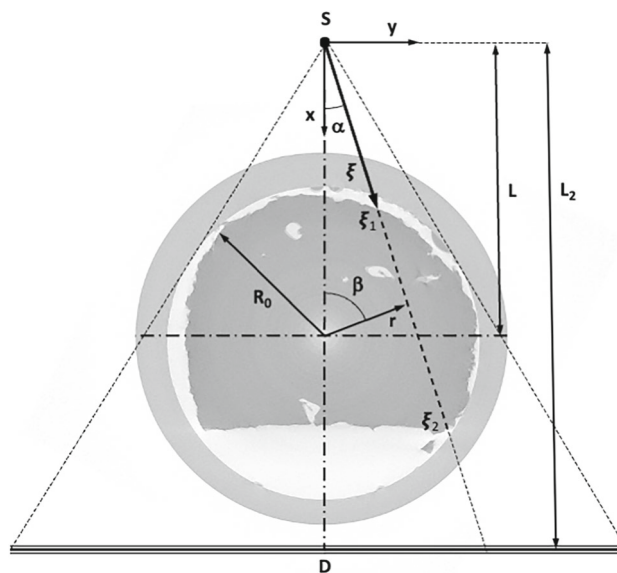
and the symmetry conditions on the axis $r = 0$ and on the plane $z = 0$ are

$$\left(\frac{\partial \chi}{\partial r} \right)_{r=0} = 0; \quad \left(\frac{\partial \chi}{\partial z} \right)_{z=0} = 0 \tag{6}$$

Equation (3) allows a separation of variables approach [4] and the general solution can be written as a series

$$\chi = \sum_{n,k=0}^{\infty} a_{n,k} e^{-D\lambda_{n,k}^2 t} J_0(\gamma_n r) \cos\left(\left(\frac{\pi}{2} + k\pi\right) \frac{z}{z_0}\right) \tag{7}$$

Fig. 3 Schematics (not to scale) of the model parameters represented on an axial slice from the X-ray 3D reconstruction of the real histological quasi-cylindrical tissue in the Eppendorf crucible; S (X-ray conical emission focal spot); D (planar X-ray digital detector); R_0 is the radius of the sample and r the general radial coordinate; L and L_2 are the distance between the X-ray source and the sample (SOD) and the distance between the X-ray source and the detector (SDD), respectively



where $\gamma_n = j_n/R_0$ and j_n are the zeroes of the Bessel function $J_0(x)$, and $\lambda_{n,k}^2 = \left(\frac{\pi}{2z_0} + k\frac{\pi}{z_0}\right)^2 + \gamma_n^2$. The BC on the sample surface (5) and the symmetry conditions (6) are satisfied by the properties of the Bessel and trigonometric functions [5]. The initial condition

$$1 = \sum_{n,k=0}^{\infty} a_{n,k} J_0(\gamma_n r) \cos\left(\left(\frac{\pi}{2} + k\pi\right) \frac{z}{z_0}\right) \tag{8}$$

can be satisfied by a proper choice of the coefficients $a_{n,k}$. These coefficients can be found using the orthogonality of the functions $J_0(\gamma_n r)$ and $\cos\left(\left(\frac{\pi}{2} + k\pi\right) \frac{z}{z_0}\right)$ (see again [5]), yielding

$$a_{n,k} = (-1)^k \frac{4}{j_n\left(\frac{\pi}{2} + k\pi\right) J_1(j_n)} \tag{9}$$

4.1 X-ray absorption

Referring to Fig. 3, the X-ray absorption for any beam crossing the sample can be calculated from the integral

$$a(\xi_1, \xi_2, t) = \int_{\xi_1}^{\xi_2} \rho(\xi, t) d\xi \tag{10}$$

where ξ is the coordinate along the beam.

In fact, using Beer’s law

$$dI = -k\rho(\xi)I(\xi)d\xi \tag{11}$$

where the local absorption coefficient is assumed to be proportional to the mass density $\rho(\xi)$, and integrating yields

$$\frac{I_e}{I_0} = e^{-k \int_{\xi_1}^{\xi_2} \rho(\xi, t) d\xi} \tag{12}$$

where I_0 is the intensity of the beam entering the sample and I_e is that of the beam exiting the sample. To calculate the integral (10) notice that $\rho = (\rho_0 - \rho_1)\chi + \rho_1$ and then

$$\int_{\xi_1}^{\xi_2} \rho(\xi, t) d\xi = (\rho_0 - \rho_1) \int_{\xi_1}^{\xi_2} \chi(\xi, t) d\xi + \int_{\xi_1}^{\xi_2} \rho_1 d\xi \tag{13}$$

Since r and z along the beam are function of ξ , using Eq. (7) yields

$$\int_{\xi_1}^{\xi_2} \chi d\xi = \sum_{n,k=0}^{\infty} C_{n,k}(\xi_1, \xi_2) e^{-D \left[\frac{1}{z_0} \left(\frac{\pi}{2} + k\pi\right)^2 + \frac{j_n^2}{R_0^2} \right] t} \tag{14}$$

where

$$C_{n,k} = a_{n,k} \int_{\xi_1}^{\xi_2} J_0\left(\frac{j_n}{R_0} r(\xi)\right) \cos\left(\left(\frac{\pi}{2z_0} + k\frac{\pi}{z_0}\right) z(\xi)\right) d\xi \tag{15}$$

so that

$$a(t) = \int_{\xi_1}^{\xi_2} \rho(\xi) d\xi = (\rho_0 - \rho_1) \sum_{n,k=0}^{\infty} C_{n,k}(\xi_1, \xi_2) e^{-D\left[\frac{1}{z_0^2}\left(\frac{\pi}{2} + k\pi\right)^2 + \frac{j_n^2}{R_0^2}\right]t} + \rho_1(\xi_2 - \xi_1) \tag{16}$$

The beam intensity reaching the X-ray detector depends on time since $a(t)$ depends on time, and from Eq. (12)

$$Y(t) = \ln\left(\frac{I_e(t)}{I_e(0)}\right) = \ln\left(\frac{-I_0k \exp(a(t))}{-I_0k \exp(a(t))}\right) = a(t) - a(0) = d_0^* + \sum_{n,k=0}^{\infty} d_{n,k}^* e^{-\frac{D}{R_0^2}\left[\frac{1}{\varepsilon^2}\left(\frac{\pi}{2} + k\pi\right)^2 + j_n^2\right]t} \tag{17}$$

where

$$d_0^* = -(\rho_0 - \rho_1) \sum_{n,k=0}^{\infty} C_{n,k}; \quad d_{n,k}^* = (\rho_0 - \rho_1) C_{n,k}; \quad \varepsilon = \frac{z_0}{R_0} \tag{18}$$

To note that the initial measurement time is different from the initial diffusion time since the sample must be positioned into the measurement region in a finite time. The substitution $t = t' + t_0$ where t' is the measuring time and t_0 is the time elapsed from the beginning of the diffusion and the beginning of measurements, Eq. (17) can be written as

$$Y(t) = c_0^* + \sum_{n,k=0}^{\infty} c_{n,k}^* e^{-\frac{D}{R_0^2}\left[\frac{1}{\varepsilon^2}\left(\frac{\pi}{2} + k\pi\right)^2 + j_n^2\right]t'} \tag{19}$$

where c_0^* is the asymptotic value of Y (i.e. when $t \rightarrow \infty$), and $c_{n,k}^*$ absorb the constant t_0 . The values of $\frac{D}{R_0^2}\left[\frac{1}{\varepsilon^2}\left(\frac{\pi}{2} + k\pi\right)^2 + j_n^2\right]$ can then be obtained by a multiple exponential fitting of $Y(t)$, even when the measured quantity is proportional to the intensity $I_u(t)$, and since all the other parameters are known, the diffusion coefficient D can be evaluated.

5 Preliminary results

As above explained it is possible to calculate an estimate of the coefficient D using the data acquired at any position in the radiographic plane.

In this *proof-of-concept* method D has been only calculated using the data acquired from the centre line of the 3 different histological quasi-cylindrical tissues (referred as sample 0, 3 and 4). To evaluate the data variability, averages over a series of ROIs (region of interest) of different sizes were used. ROI of 160×160 , 80×80 and 54×54 pixels (matching by calibration to 0.81×0.81 , 0.40×0.40 and 0.27×0.27 mm², respectively) were used to evaluate the effect of ROI size on the D estimation for sample 0.

From each ROI, an average of the X-ray attenuation intensities can be obtained, and a fitting of the 4-terms truncated series (19) was used to calculate D , and the results are shown in Fig. 4.

The estimated value of D , which should be expected to be roughly uniform throughout the whole sample volume, shows an overall consistency with a variability that increases towards the sample edge. Which is due to the tangentiality of X-rays which passes through increasingly smaller thicknesses of the sample and therefore reduces the attenuation to values that are barely distinguishable from the background noise, with a lower average value. The estimated value of D for the 3 different samples and ROI of 0.40×0.40 is plotted in Fig. 5.

The average value of D in the sample inner core is 3.2×10^{-9} m²/s, with relative standard deviation of about 6%, while that in the outer part of the sample is 2.4×10^{-9} m²/s with standard deviation of about 20% as per above commented. This discrepancy can be ascribed to many reasons, among which the assumptions of uniformity of the sample and of cylindrical symmetry are possibly the most questionable. On the one hand, an analysis of the sample evidence that regions of vascularization are present, thus weakening the uniformity assumption. The assumption of cylindrical symmetry is not fully justified since, as evidenced in Fig. 3, in carrying out the experiments, a limited removal of material on one side was necessary to allow the flushing of the solvent also in the Eppendorf crucible.

Despite of all that the measured value of the average diffusion coefficient is consistent in the order of magnitude with the prudential values referred to in the literature [6]. A diffusion velocity equal to 0.7 mm/h is often proposed as a rough estimation for alcohol, however poorly documented and substantially underestimated, and the value obtained from the measurements (as $V = D/L$, where L is the sample size) is around 1.3 mm/h, thus consistent with the order of magnitude.

Fig. 4 Estimated value of D for different ROIs in the same histological quasi-cylindrical tissue sample 0, from the centre line and at different radial distances (r)

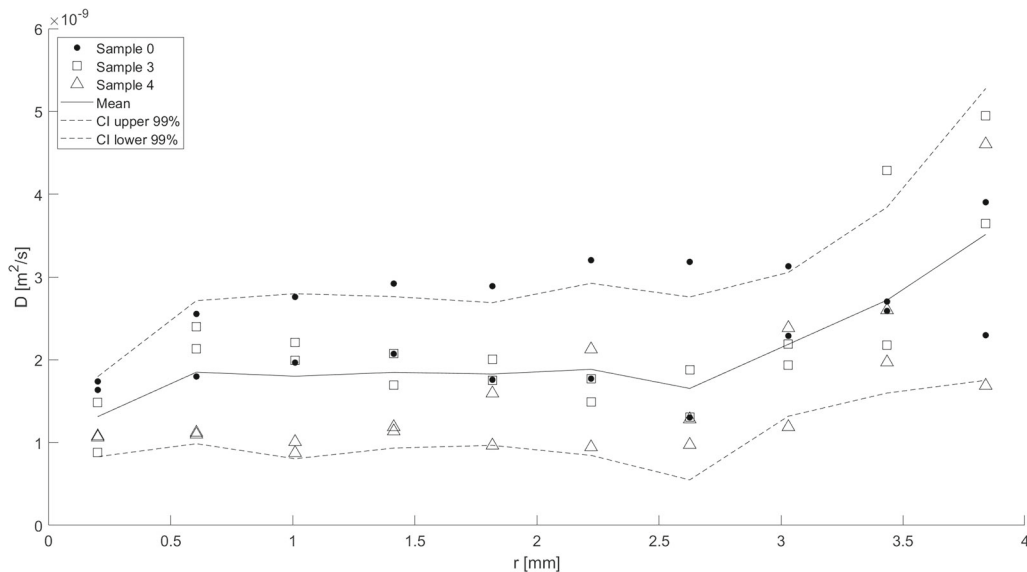
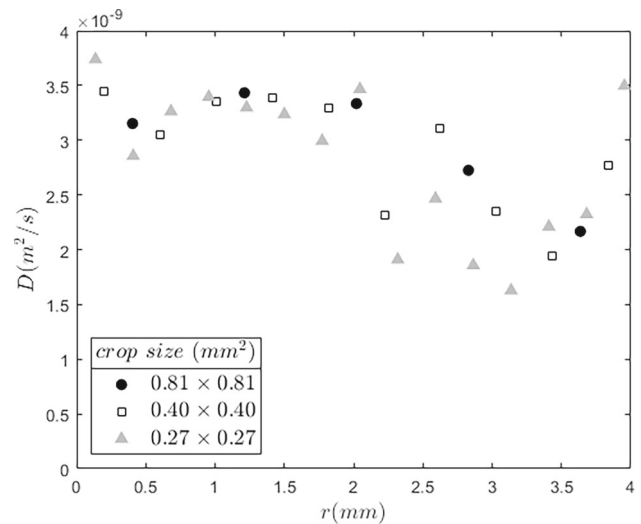


Fig. 5 Estimated value of D for 3 different histological quasi-cylindrical tissues (sample 0, 3 and 4), from the centre line of the sample and at different radial distances (r) compared to the global 99% confidence interval (CI)

The results of this first attempt to apply the X-ray microCT method for measuring the effective diffusion coefficient of a solvent in a histological sample are encouraging, and in the next future some of the above-mentioned weakness will be relieved by a more accurate modelling approach.

6 Conclusions

The estimates of the value of the diffusion coefficient D , obtained by the method based on the sequential registration of high-resolution radiographic images of histological quasi-cylindrical tissues during the perfusion of a solvent over time, were found to be consistent with the best-practice in histological preparation processes. The technique is novel, is relatively independent of the size of the analysed sample thus adapting to the typical arbitrary resections obtained from biopsies. The authors are confident that this *proof-of-concept* can be further refined to allow for optimised tissue sample processing, permitting a more accurate definition of solvent processing times, with consequent limited sample deterioration that often results in a compromised diagnostic quality.

Acknowledgements This work was funded by the Italian National Plan for NRRP Complementary Investments (PNC, established with the decree-law 6 May 2021, n. 59, converted by law n. 101 of 2021) in the call for the funding of research initiatives for technologies and innovative trajectories in the health and care sectors (Directorial Decree n. 931 of 06-06-2022)-project n. PNC0000003-AdvaNced Technologies for Human-centred Medicine (project acronym:

ANTHEM). This work reflects only the authors' views and opinions, neither the Italian Ministry for University and Research nor the European Commission can be considered responsible for them.

Authors wishing to acknowledge bachelor students (in alphabetical order) E. Lenzi, A. Mamoli, E. Medolago, C. Sirtoli.

Funding Open access funding provided by Università degli studi di Bergamo within the CRUI-CARE Agreement. Funding was provided by the PNC (Italy) (Grant No. PNC0000003).

Data Availability Statement No data associated in the manuscript.

Declarations

Conflict of interest The author declare that they have no conflict of interest.

Open Access This article is licensed under a Creative Commons Attribution 4.0 International License, which permits use, sharing, adaptation, distribution and reproduction in any medium or format, as long as you give appropriate credit to the original author(s) and the source, provide a link to the Creative Commons licence, and indicate if changes were made. The images or other third party material in this article are included in the article's Creative Commons licence, unless indicated otherwise in a credit line to the material. If material is not included in the article's Creative Commons licence and your intended use is not permitted by statutory regulation or exceeds the permitted use, you will need to obtain permission directly from the copyright holder. To view a copy of this licence, visit <http://creativecommons.org/licenses/by/4.0/>.

References

1. R. Haide, S. Fest-Santini, M. Santini, Use of X-ray micro-computed tomography for the investigation of drying processes in porous media: a review. *Drying Technol.* **40**, 1731–1744 (2022)
2. J. Crank, *The mathematics of diffusion* (Clarendon Press Series, University of Oxford, 1979)
3. M. Santini, S. Fest-Santini, P. Foltyn, On the local mass transfer rates around arbitrary shaped particles calculated by X-ray computed microtomography: prospective for a novel experimental technique. *Int. Commun. Heat Mass Transfer* **79**, 135–139 (2016)
4. M.S.P. Moon, D.E. Spencer, *Field theory handbook*, 2nd edn. (Springer-Verlag, Berlin, 1988)
5. F.W.J. Olver, D.W. Lozier, R.F. Boisvert, C.W. Clark (eds.), *NIST handbook of mathematical functions* (Cambridge University Press, Cambridge, 2010)
6. W. Saltzman, *Diffusion in biological systems in drug delivery: Engineering principles for drug therapy* (Oxford Academic, New York, 2001)